Chapter 10
Kinetic Modeling of *E. coli* Enzymes: Integration of *in vitro* Experimental Data

Ekaterina A. Mogilevskaya, Kirill V. Peskov, Eugeniy A. Metelkin, Galina V. Lebedeva, Tatiana Y. Plyusnina, Igor I. Goryanin, and Oleg V. Demin

Contents

Abstract The metabolic network of *E. coli* is one of the most well studied biochemical systems, with an abundance of *in vitro* and *in vivo* data available for quantitative estimation of its kinetic parameters. In this chapter, we present our approach to developing mathematical description of individual enzymatic reactions within bacterial metabolic networks. This description is based on the detailed consideration of enzyme catalytic mechanisms and includes several stages: reconstruction of the enzyme catalytic cycle, derivation of the reaction rate equation, and validation of its parameters on the basis of available *in vitro* experimental data. We illustrate our strategy with the models developed for three *E. coli* enzymes with rather complicated regulatory mechanisms: allosteric tetramer phosphofructokinase-1, citrate synthase with its regulation by ATP and pH, and β-galactosidase validated against time dependencies of its substrates. The modeling results clearly demonstrate that developing detailed enzyme kinetic models is essential to capture key regulatory properties of enzymes. The kinetic models allow to integrate large sets of *in vitro*

I.I. Goryanin (✉)
Centre for Systems Biology, University of Edinburgh, Edinburgh, EH9 3JU, 0131 6519063 Scotland, UK; Informatics Forum, University of Edinburgh, Edinburgh, EH8 9LE Scotland, UK
e-mail: goryanin@inf.ed.ac.uk

S.Y. Lee (ed.), *Systems Biology and Biotechnology of Escherichia coli*,
DOI 10.1007/978-1-4020-9394-4_10,

experimental data available for *E. coli* enzymes and to get insight into important regulatory features of their catalytic mechanism.

10.1 Introduction

The last several years have seen substantial progress in molecular biology and genetic research of *E. coli* (Han and Lee 2006, Ishii et al. 2007, Perna et al. 2001). Sequence information on the genomes of hundreds of different organisms has stimulated the emergence of functional genomics, a discipline that sets out to understand the meaning of sequenced data using high throughput small molecule, gene and protein expression data. Life scientists have transformed old-style protein chemistry into proteomics, and traditional biochemistry into metabolomics. These new fields provide essential clues to the underlying metabolic, gene regulatory and signaling networks that operate in cells, tissues and organisms under different conditions.

Cellular metabolism of *E. coli*, the integrated interconversion of more then two thousands of metabolic substrates through more then one thousand enzyme-catalyzed biochemical reactions, is the most investigated system of intracellular molecular interactions (Feist et al. 2007). When one has knowledge of most, or all, of the major biological entities and stoichiometry of their interactions an illusion could appear that this voluminous knowledge will enable us to predict whole cell behavior for the purposes of mechanistic understanding and bioengineering control. Indeed, in some cases, it is possible to make plausible predictions based on "static" non temporal information without relying upon kinetic data (Edwards et al. 2001, Kim et al. 2008, Price et al. 2004, Schütz et al. 2007). Recently, stoichiometric metabolic models (SMM) and metabolic engineering techniques have been successfully applied to improve production of succinic acid, lactic acid, L-threonine, and L-valine by *E. coli*. (Lee et al. 2007, Lee et al. 2005, Park et al. 2007). Unfortunately, SMM techniques cannot predict cellular bahaviour in non-steady state conditions. It results in high level of false positive predictions (Lee et al. 2006). Time series data cannot be easily integrated to SM models as well, so it is difficult to validate SM models, as steady state or chemostat cultures are reqired. It is difficult to incorporate to SMM real data from batch or fed batch experiments, and time series after systems perturbations (immediately or short after the intervention) (Ishii et al. 2007).

The discrepancy between SMM predictions and experimental data is usually explained by the statement that ultimately the real cell will mimic *in silico* behavior after process of evolution. But, the questions why and how the process of evolution itself is happening, which physico-chemical properties of proteins are subject of selective pressure are not addressed at all.

Indeed, overall cellular behavior is determined not only by available biological entities, but mainly by their dynamic interactions and individual properties. Activities of most if not all of the enzymes involved in cellular metabolism are often regulated by the end products and intermediates of corresponding pathways. This complex network of positive and negative feedbacks, as well as genetic regulation of expression levels, provides flexible adaptation of the metabolic network to fast

and slow changes in environmental conditions. It is the overall dynamic nature of the whole cell that determines not only its present properties, but its future ones as well. The cellular regulatory system is responsible for maintenance of homeostasis and for transitions between different physiological states. That is why when modeling cellular metabolism, it is essential to consistently describe its key regulatory properties. The regulatory system of *E. coli* metabolism is known to have an hierarchical architecture, including regulatory effects at the levels of enzyme activity, gene transcription and translation. Consistent mathematical description of this complex multilevel regulatory system requires accurate consideration of the regulatory properties of individual components involved in the metabolic network – enzymes, which further contribute to the regulatory properties of the whole system. This task becomes extremely important with the recent expansion of a new discipline – synthetic biology, the ultimate goal of which is to design and build engineered biological systems with predefined properties (Barrett et al. 2006, Endy 2005).

In this paper we present kinetic modelling approach applied to modeling the individual enzymatic reactions within metabolic networks of *E. coli*, which allows capture of the key regulatory properties of these networks. Our approach is based on the detailed consideration of the enzyme catalytic cycle and on the utilization of all available experimental data characterizing the kinetics of the enzyme being studied. This modeling approach includes several stages. The first is the reconstruction of a catalytic cycle of the enzymes. This cycle represents both interaction of the enzyme with substrates and products and the effect of different inhibitors and activators. The second stage is the derivation of the reaction rate equation that defines quantitative dependence of the rate of the enzyme performance on concentrations of substrates, products and effectors. The third and last stage is the identification of the parameters for into the rate equation based on the available experimental data. To illustrate our approach and its stages, as well as to demonstrate how different types of experimental data can be incorporated into the kinetic model, we present our developed kinetic models for several *E. coli* enzymes which are known to have complicated patterns of regulation of their activity: phosphofructokinase 1, β-galactosidase and citrate synthase.

10.2 Methods

10.2.1 Basic Principles of Kinetic Description of Enzymatic Reactions Using In Vitro *Experimental Data*

As a part of our strategy to make the models scalable and comparable with different kinds of experimental data, we develop both *detailed* and *reduced* descriptions for every appropriate biochemical process to make the models scalable and comparable with different kinds of experimental data. The *detailed* reaction description includes the exact molecular mechanism of the reaction, i.e. enzyme catalytic cycle. Usually, the detailed kinetic model of an enzyme reaction represents a set of ordinary differential equations describing the totality of elementary reactions within the enzyme

catalytic cycle, such as substrate binding, catalytic transformation of substrates into products, product release, etc. It defines the dynamics of all possible enzyme intermediate states (free enzyme, enzyme-substrate, enzyme-product complexes), as well the time course of substrates and products consumption/production. The *reduced* description represents the reaction rate as an explicit analytic function of the concentration of substrates and products.

In our approach, for each active protein involved in the model of metabolic network, i.e. enzyme with catalytic function, we identify from the literature or hypothesize the catalytic cycle based on 3D structures and other relative biological information. Basing on the developed scheme of the catalytic mechanism we can construct a detailed kinetic model of the enzyme catalytic cycle. In most cases such a detailed model can further be replaced with a reduced description of the reaction rate. To derive the corresponding rate equations from the catalytic cycle, we use quasi-steady state and rapid equilibrium approaches (Demin and Goryanin 2008). The catalytic cycle of each enzyme is described by non-linear differential equations. Initially, concentrations of substrates, products and effectors (inhibitors and activators) are assumed to be buffered, i.e. do not change with time.

The quasi-steady state of the system is calculated as a function of substrates, products, inhibitors, activators, total protein concentrations and all kinetic constants of the processes. The rate law for every process is derived as a flux from the catalytic cycle for this quasi-steady state. Finally, the rate law depends on temporal changes of the total concentration of the protein, concentrations of the effectors (activators, inhibitors, agonists, and antagonists), substrates, products and the values of the kinetic parameters (K_m, K_i, K_d and elementary rate constants).

The level of detailed elaboration of the catalytic cycles of selected enzymes and subsequent derivation of rate equations are fully determined by the available experimental data on the structural and functional organization of the enzyme. Indeed, if the catalytic cycle of the enzyme is established and proved experimentally then we use it to derive the rate equation. If the mechanism underlying enzyme operation is unknown we infer a “minimal” catalytic cycle that

1. satisfies all structural and stoichiometric data available from literature
2. allows us to derive a rate equation describing all available kinetic experimental data
3. is the mathematically simplest catalytic cycle of all possible ones satisfying clauses 1 and 2.

Another challenge in developing a mathematical description of enzyme catalysis based on *in vitro* data is that the kinetic experimental data available from literature are usually obtained under different conditions (pH, temperature). This means that we should account for these parameters in our model, i.e.

4. construct such a catalytic cycle and derive such a rate equation that satisfies available experimental data describing the dependence of enzyme activity on pH, temperature and other experimental conditions

5. the mechanism describing the dependence of the reaction rate on pH and temperature should be taken into account in the catalytic cycle of the enzyme in the simplest of all possible ways

Parameter estimation is the third stage of model development. To estimate the kinetic parameter values we use the following sources:

1. literature data on the values of K_m, K_i, K_d, rate constants, pH optimum, etc;
2. electronic databases; only a few databases with specific kinetic content are available at the moment, in particular EMP (Selkov et al. 1996) and BRENDA (Shomburg et al. 2002)
3. Experimentally measured dependencies of the initial reaction rates on concentrations of substrates, products, inhibitors and activators
4. Time series data from enzyme kinetics

However, many processes, such as enzyme reactions, have not been studied kinetically. Moreover, many kinetic parameters cannot be estimated from the literature or databases due to a lack of available experimental data. One remedy is to express these unknown or "free" parameters via other available measured kinetic parameters. The result is the establishment of functional relationships between "free" parameters and measured kinetic parameters. Each parameter value, of course, is constrained by physico-chemical properties and any other information available from other organisms or related processes. The more constraints available, the more defined is the system.

To illustrate the basic principles of construction of catalytic cycles and derivation of rate equations described above we present the results of the modeling of three enzymes of *E. coli* metabolism: phosphofructokinase-1, β-galactosidase and citrate synthase. We demonstrate how kinetic data measured at different conditions (pH, temperature and others) can be taken all together to construct a quantitative description of enzyme catalytic activity and its regulation. The method developed in this section allows us to predict kinetic behaviour of the enzymes at any set of experimental or cellular conditions.

10.3 Results

10.3.1 Kinetic Modeling of Phosphofructokinase-1 (pfkA) from E. coli Cells

Phosphofructokinase-1 (PfkA) catalyzes the transfer of γ-phosphate from ATP to fructose-6-phosphate (F6P) resulting in ADP and fructose-1,6-biphosphate (F16bP) production (Babul 1978, Blangy et al. 1968, Kotlarz and Buc 1982):

$$ATP + F6P \xrightarrow[Mg^{2+}]{PfkA} ADP + F16bP$$

This reaction is of importance in regulation of glycolysis and gluconeogenesis (Ausat et al. 1997, Babul 1978, Berger and Evans 1991, Blangy et al. 1968, Deville-Bonne et al. 1991a, Deville-Bonne et al. 1991b, Kotlarz and Buc 1982, Rye et al. 1995, Saier and Ramseier 1996, Saier et al. 1996, Waygood and Sanwal 1974). *E. coli* cells contain two isozymes of this enzyme: PfkA and PfkB (Babul 1978, Kotlarz and Buc 1982). PfkA, studied in this work, is considered to be a key phosphofructokinase in *E. coli* metabolism (Kotlarz and Buc 1977, Torres and Babul 1991, Vinopal and Fraenkel 1974, 1975).

Unlike PfkB, PfkA has a rather complicated regulatory profile: purine nucleotide diphosphates, ADP (Babul 1978, Blangy et al. 1968, Kotlarz and Buc 1982) and GDP (Ausat et al. 1997), are acting as activators, phosphoenolpyruvate (PEP) is the inhibitor (Babul 1978, Blangy et al. 1968, Kotlarz and Buc 1982). In this case, all the regulators of this enzyme are allosteric, by virtue of the fact that binding sites found for effectors do not overlap with catalytic ones (Reeves and Sols 1973). Moreover, phosphorylation of fructoso-6-phosphate is carried out in the presence of Mg^{2+} ions (Babul 1978, Blangy et al. 1968, Kotlarz and Buc 1982).

The evidence in favor this protein being an allosteric enzyme is as follows: the quaternary structure of the enzyme (tetramer); complex regulatory profile due to the presence of complementary allosteric sites at the monomer; and sigmoid dependencies of initial rates of the reaction on F6P concentrations (Babul 1978, Blangy et al. 1968, Kurganov 1978).

In this part we constructed the kinetic model of phosphofructokinase-1, that describes the majority of the experimental data known for this enzyme. This model examins the properties of phosphofructokinase-1 such as substrate and product inhibition, cooperativity and competition at joint action of allosteric effectors.

10.3.1.1 Catalytic Cycle of Phosphofructokinase-1 Construction

An approach to modeling the kinetics of allosteric enzymes has been developed by Monod, Wyman, Changeux (MWS) (Monod et al. 1965) and it is traditionally used by a majority of modellers. At the same time this modeling approach is valid only for the enzymes which catalyze the reactions of irreversible isomerization, since enzyme-binding of only one substrate is taken into account and the catalytic stage is thought to be irreversible. Moreover, MWS-based modeling includes several strong assumptions that make it practically impossible to use it while modeling real enzymes (Kurganov 1978). There exist a number of generalizations for the MWS-based modeling techniques, which allow the inclusion of allosteric regulation in models of enzymes with more complicated mechanisms. We took a generalization offered in (Ivanitsky et al. 1978), which assumes that the enzyme can exist in two states: R (relaxed) and T (tense). Unlike standard MWS-based modeling, in this approach the functional difference between R and T states is not only in different affinities of substrates, products and effectors with respect to the enzyme, but also in the catalytic properties of these states. In other words, not only Michaelis constants and dissociation constants as in MWS-based modeling (Monod et al. 1965), but also catalytic constants (Deville-Bonne et al. 1991b) are different for R and T states. One

another important difference is as follows: a catalytic cycle of separate subunits is taken into consideration in the generalization alluded. This gives us a possibility to take into account detail kinetic mechanism of an enzyme and estimate a contribution of product inhibition.

The rate of reaction may be modulated by variation of the relationship between the states of the enzyme. By this means allosteric regulation is introduced, since enzyme-binding of the effectors in a site, which is separate from catalytic one, will disturb the equilibrium. For instance, activators (that demonstrate the best affinity to R-form) shift the balance to the R-state; and vice versa, inhibitors (which bind more with the T-form) shift the balance to the T-state. In this case, the action of the effectors (activation or inhibition) will be determined only by the ratio of dissociation constants of different forms of the enzyme (Kurganov 1978). The existing experimental data on regulation of phosphofructokinase-1 hold that its regulation is carried out in just this manner, since binding sites both for PEP, and for ADP (GDP), have been found separately from the catalytic cycle (Ausat et al. 1997, Babul 1978, Blangy et al. 1968, Reeves and Sols 1973).

Catalytic Cycle of Separate Subunit

Since we have found no unambiguous opinions as to the mechanism of action of a single subunit in the literature on phosphofructokinase-1, we proposed that the monomer of phosphofructokinase-1 and its isozyme PfkB have a similar mechanism of action. In (Campos et al. 1984) the monomer of phosphofructokinase-2 was shown to operate by the mechanism of Ordered Bi Bi, in accordance with the classification offered by Cleland (Cleland 1963). First F6P and then ATP binds with the enzyme resulting in phosphorylation (Campos et al. 1984, Ewings and Doelle 1980, Guixe and Babul 1985). Furthermore, as $ATPMg^{2-}$ was a substrate of the reaction, we added to the catalytic cycle a competitive inhibition of the free form of ATP^{4-}. This inhibition can be registered when the complete ATP concentration increases in a system with a fixed Mg^{2+} concentration. The pH effect on the activity of the enzyme has been taken into account in a standard way suggested by Cornish-Bowden (Cornish-Bowden 2001), as was shown for the *E. coli* enzyme imidazole glycerol phosphate synthase (Demin et al. 2004). Having summarized the above material, it is possible to construct the profile of the catalytic cycle of a separate subunit of phosphofructokinase-1.

10.3.1.2 Derivation of the Rate Equation of Phosphofructokinase-1

The rate equation, a generalization of MWS modeling by Popova and Sel'kov for multisubstrate reactions is written as follows (Ivanitsky et al. 1978):

$$\begin{aligned} V &= n \cdot f \left(1 + ({}^{f'}\!/_{f})Q\right)/(1+Q) \\ Q &= L_0 \left(\frac{\left(1 + {}^{I}\!/_{K_i^t}\right)}{\left(1 + {}^{I}\!/_{K_i^r}\right)} \cdot \frac{E_r}{E_t} \right)^n \end{aligned} \tag{10.1}$$

where f is the rate equation derived on the basis of catalytic cycle of single subunit in r-state, f' – the rate equation derived on the basis of catalytic cycle of single subunit in t-state, E_r – concentration of free enzyme in r-state, E_t – concentration of free enzyme in t-state, L_0 – constant equilibrium for r/t-transition, I – allosteric effecter, n – number of enzyme's subunits.

Q is a function of a state, it determines the relation between R and T forms of the enzyme. In order to write the function of a state of the enzymes under study, we should, in accordance with a regulatory profile, take into account the action of all allosteric effectors (Ivanitsky et al. 1978, Kurganov 1978):

$$
\begin{aligned}
f &= \frac{V_{mr}^{forward} \cdot \left(ATPMg^{2-} \cdot F6P - ADPMg^{-} \cdot F16bP / Keq \right)}{Z_{SP}^{R} \cdot Z_{pH}}; \\
Z_{pH} &= 1 + H^{+} / K_{d\_H\_1} + K_{d\_H\_2} / H^{+}; \\
Z_{SP}^{R} &= K_{ir\_F6P} \cdot K_{mr\_ATPMg^{2-}} + K_{mr\_ATPMg^{2-}} \cdot F6P \cdot \left(1 + \frac{ATP^{4-}}{K_{ir\_ATP^{4-}}} \right) + \\
&\quad + K_{mr\_F6P} \cdot ATPMg^{2-} + ATPMg^{2-} \cdot F6P + \\
&\quad + K_{mr\_F6P} \cdot ATPMg^{2-} \cdot FbP / K_{ir\_FbP} + \\
&\quad + ATPMg^{2-} \cdot F6P \cdot ADP / K_{ir\_ADP} + \\
&\quad + K_{mr\_F6P} \cdot ATPMg^{2-} \cdot ADP \cdot FbP / Wr \cdot K_{mr\_ADP} \cdot K_{ir\_FbP} + \\
&\quad + Wr / Keq \cdot \left(\begin{array}{c} K_{mr\_FbP} \cdot F6P \cdot ADP / K_{ir\_F6P} + K_{mr\_ADP} \cdot FbP + \\ + K_{mr\_FbP} \cdot ADP + ADP \cdot FbP \end{array} \right);
\end{aligned}
\tag{10.2}
$$

f is the rate equation derived on the basis of catalytic cycle of a single subunit. The expression of reaction rate (the reaction runs by the mechanism of Ordered Bi Bi), borrowed from Cleland (Cleland 1963), was slightly modified, and competitive inhibition of ATP^{4-} and pH effects were added. Moreover, experimental findings suggest that the reaction, catalyzed by phosphofructokinase-1, is virtually irreversible (Babul 1978):

$$
Keq = Wr \frac{K_{ir\_F6P} \cdot K_{mr\_ATPMg^{2-}}}{K_{ir\_FbP} \cdot K_{mr\_ADP}} = Wt \frac{K_{it\_F6P} \cdot K_{mt\_ATPMg^{2-}}}{K_{it\_FbP} \cdot K_{mt\_ADP}} \tag{10.3}
$$

An expression for f' appears in much the same manner, with the only difference from f that the expression for f' contains the constants of binding and catalytic constants of the T-state.

Er and *Et* is the expression for a free form of the enzyme in R-and T-states (Ivanitsky et al. 1978), respectively:

$$
\begin{aligned}
Q &= Lo\left(\frac{\left(1+\frac{ADP}{K_{eft\_ADP}}+\frac{GDP}{K_{eft\_GDP}}\right)\left(1+\frac{PEP}{K_{eft\_PEP}}\right)}{\left(1+\frac{ADP}{K_{efr\_ADP}}+\frac{GDP}{K_{efr\_GDP}}\right)\left(1+\frac{PEP}{K_{efr\_PEP}}\right)}\frac{E_r}{E_t}\right)^n \\
Er &= \frac{K_{ir\_F6P}\cdot K_{mr\_ATPMg^{2-}}\cdot Eo}{Z_{SP}^R} \\
Et &= \frac{K_{it\_F6P}\cdot K_{mt\_ATPMg^{2-}}\cdot Eo}{Z_{SP}^T}
\end{aligned}
\tag{10.4}
$$

Substitution of expressions (10.2, 10.3, and 10.4) in (10.1) gives a complete equation of the rate of a reaction, catalyzed by phosphofructokinase-1.

10.3.1.3 Estimation of the Parameters of the Rate Equation of Phosphofructokinase-1

As a result of the above, the model contains 20 parameters, two of which we could take from the literature data – $Kd\_ATPMg = 0.0588$ (Taquikhan and Martell 1962), $w\_pfk1 = 0,08$ (Babul 1978). In order to determine the remaining parameters appearing in the rate equation, we fitted the model with experimental data. In total, the 11 experimental curves published in (Ausat et al. 1997, Babul 1978, Deville-Bonne et al. 1991a) were used to determine 18 parameters. It should be noted that the curves obtained in our model correlate rather well with the experimental data (Figs. 10.1a–d, and 10.2a). In addition, the obtained parameter values and analysis of behavior of the model may lead to the following conclusions:

1. Phosphofructokinase-1 has a distinct allostericity associated with different affinities of substrates to states of the enzyme. At the same time, the difference between Michaelis constants of R- and T-states reaches several orders. The above has a great influence on the shape of the curves of initial reaction rate dependence on substrate concentrations (Figs. 10.1b, and 10.2a).
2. Figure 10.2a clearly shows that substrate inhibition appears in the experimental *in vitro* system at a total ATP concentration of more than 10 mM and at a fixed concentration of Mg^{2+} ions (10 mM); at a total ATP concentration of 20 mM, the phosphofructokinase reaction rate in the *in vitro* system is only 20% of the maximum. The mechanism of this inhibition is coupled with emergence in the system of a free form, ATP^{4-} (Fig. 10.2b), which, as mentioned above, acts as an inhibitor by competing with the substrate, magnesium form $ATPMg^{2-}$, for the catalytic site. The values of identified parameters also point to a possibility of substrate inhibition (Table 10.1). So, the ATP^{4-} molecule free from magnesium ions has better affinity to the enzyme than the magnesium form.

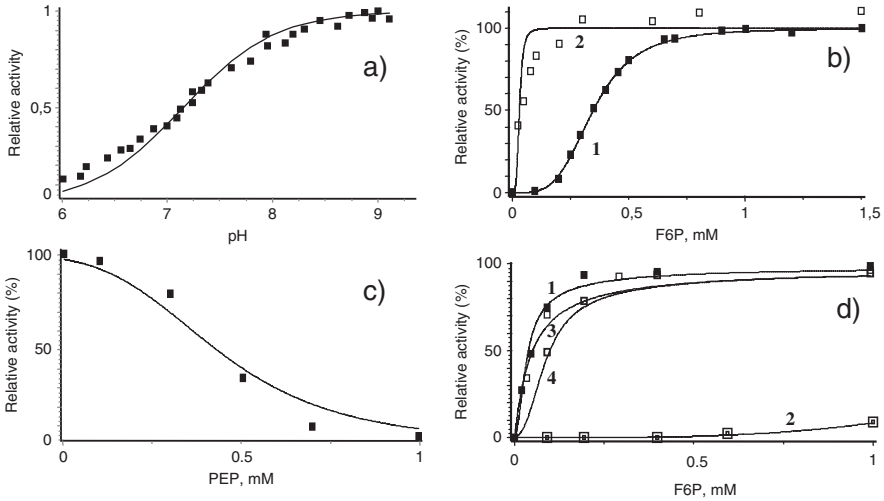

Fig. 10.1 The comparison of experimental data on PfkA-1 and model results. (**a**) PfkA relative maximal activity dependence on pH described by the model and experimental data (Park et al. 2007); (**b**) PfkA relative activity dependence on F6P concentration described by the model and experimental data (Barrett et al. 2006): curve 1 (■) – ATP = 1 mM, Mg^{2+} = 10 mM, GDP = 0 mM, pH = 8.2; curve 2 (□) – ATP = 1 mM, Mg^{2+} = 10 mM, GDP = 2 mM, pH = 8.2; (**c**) PfkA relative activity dependence on PEP concentration described by the model and experimental data (Lee et al. 2005): ATP = 1 mM, Mg^{2+} = 10 mM, F6P = 1 mM, pH = 8.2; (**d**) PfkA relative activity dependence on F6P concentration described by the model and experimental data (Lee et al. 2005): curve 1 (■) – ATP = 1 mM, Mg^{2+} = 10 mM, ADP = 0.5 mM, PEP = 0 mM, pH = 8.2; curve 2 (⊡) – ATP = 1 mM, Mg^{2+} = 10 mM, ADP = 0 mM, PEP = 1 mM, pH = 8.2; curve 3 (□) – ATP = 1 mM, Mg^{2+} = 10 mM, ADP = 1 mM, PEP = 0.1 mM, pH = 8.2; curve 4 (◘) – ATP = 1 mM, Mg^{2+} = 10 mM, ADP = 1 mM, PEP = 1 mM, pH = 8.2

3. Another property of phosphofructokinase-1, the significant effect of which on the kinetic curves we have shown, is that, besides allosteric ADP activation, there is an apparent product inhibition by this metabolite. In other words, ADP can compete with ATPMg^{2+} for the catalytic site. Although product inhibition has no effect on reaction rate that would be noticeable under experimental conditions, it shows up in the combined action of allosteric effectors (curves 2, 3, 4 on Fig. 10.1d). Parameter values obtained from fitting also suggest the possibility of significant inhibition by ADP. So, $Kmr\_ADP = 0.69$ mM, evidencing fair affinity of ADP molecule to phosphofructokinase-1.
4. The analysis of fitted parameter values for the binding of effectors in allosteric sites shows that the activators ADP and GDP bind almost exclusively with the R-state of the enzyme, while the inhibitor PEP binds with the T-state. This proves that any significant synergy due to a combined action of allosteric effectors is impossible, because it is impossible for antagonistic regulators to bind simultaneously with a single subunit.
5. Activation of phosphofructokinase-1 by GDP (Fig. 10.2b) is probably also modulated by competitive inhibition, provided that GDP is bound in the catalytic

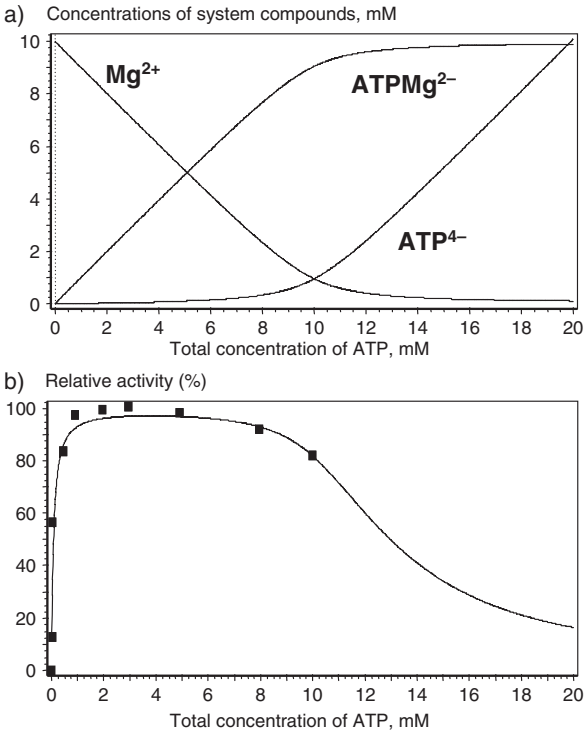

Fig. 10.2 Effect of PfkA inhibition by ATP^{4-}. (**a**) ATP^{4-}, Mg^{2+} and $ATPMg^{2-}$ concentration dependence on the total ATP concentration; (**b**) PfkA relative activity dependence on the total ATP concentration described by the model and experimental data (Lee et al. 2005): F6P = 1 mM, Mg^{2+} = 10 mM, pH = 8.2

site instead of $ATPMg^{2+}$. Such a situation is observed in some kinases that use different nucleotide phosphates in their action, e.g., pyruvatekinase-1 from *E. coli* (Waygood and Sanwal 1974). Most probably, GDP and ADP are bound in the same regulatory site (Ausat et al. 1997), therefore competition is possible in the presence of two effectors in the medium. The results of fitting (Table 10.1) show that ADP has nearly two times better affinity to the allosteric site than GDP: $Kir\_ADP = 0.0737$ mM, whereas $Kir\_GDP = 0.122$ mM. However, the absence of experimental data prevents any unambiguous conclusions.

10.3.2 The Kinetic Model of β-galactosidase from E. coli *Cells*

β-galactosidase (EC 3.2.1.23) is an important enzyme of *Escherichia coli* involved in sugar utilization. Together with lac-permease, this protein is encoded in the region of the lac-operon, which is the most popular model system for the study of transcription regulation in prokaryotes.

The enzyme has a complex catalytic cycle and catalyzes several reactions in a single catalytic site. As has been shown previously, the main catalytic activity of β-galactosidase at the addition of lactose to the medium reverts to hydrolysis of the latter with the formation of glucose and galactose monosaccharides (Huber

Table 10.1 PfkA model parameters values estimated from experimental data

Model parameter	Value (mM)	Reference
Kmr_ATPMg	8.13e-05	(Kim et al. 2008, Lee et al. 2006)
Kmr_F6P	2.05e-05	(Kim et al. 2008, Lee et al. 2006)
Kir_F6P	1.84	(Kim et al. 2008, Lee et al. 2006)
Kir_ATP	3.17e-05	(Kim et al. 2008, Lee et al. 2006)
Kefr_PEP	200	(Kim et al. 2008)
Kefr_ADP	7.37e-02	(Kim et al. 2008)
Kefr_GDP	0.197	(Lee et al. 2006)
Kir_FbP	2.58e-02	(Kim et al. 2008)
Kmr_FbP	5.5	(Kim et al. 2008)
Kir_ADP	1000	(Kim et al. 2008)
Kmr_ADP	0.69	(Kim et al. 2008)
Kmt_ATPMg	3.35	(Kim et al. 2008, Lee et al. 2006)
Kit_ATP		
Kmt_F6P	780	(Kim et al. 2008, Lee et al. 2006)
Kit_F6P		
Keft_PEP	33.1	(Kim et al. 2008, Lee et al. 2006)
Keft_ADP		
Keft_GDP	8.56e-03	(Kim et al. 2008, Lee et al. 2006)
Kit_FbP	2.6e-01	(Kim et al. 2008)
Kmt_FbP	1	(Kim et al. 2008)
Kmt_ADP	61	(Lee et al. 2006)
Kit_ADP	143	(Kim et al. 2008)
Lo	660	(Kim et al. 2008)
Kd_H_1	1e+03	(Kim et al. 2008)
Kd_H_2	1e+03	(Kim et al. 2008)
	14.4	(Kim et al. 2008, Lee et al. 2006)
	3.78e-12	(Park et al. 2007)
	6.97e-05	(Park et al. 2007)

et al. 1976), as well as reaction of isomerization with the formation of allolactose (Burstein et al. 1965, Jobe and Bourgeois 1972). This work (Huber et al. 1976) has also shown that a certain amount of tri- and tetrasaccharides appear in the medium.

In this section we have constructed a kinetic model of β-galactosidase, which describes both hydrolysis and transgalactosidase activity of the enzyme. On the basis of experimental data available currently, kinetic parameters of the model have been found. Using the constructed model, we analysed correlation between different enzyme activities under different conditions.

10.3.2.1 Construction of β-galactosidase Catalytic Cycle

The catalytic cycle of *E. coli* β-galactosidase (Fig. 10.3) was constructed based on the scheme proposed in (Huber et al. 1976), extended by the addition of trisaccharide formation stages. The scheme describes both hydrolase and transgalactosidase activities of β-galactosidase. Stages 1a and 2a show the binding of lactose (*lac*) and allolactose (*alac*), respectively, with the catalytic center of free enzyme (*E*) with the formation of enzyme-substrate complex (*E_lac* and *E_alac*, respectively). Stages 1b and 2b describe decomposition of disaccharides to glucose and galactose in the catalytic center of the enzyme, which results in the formation of a ternary complex

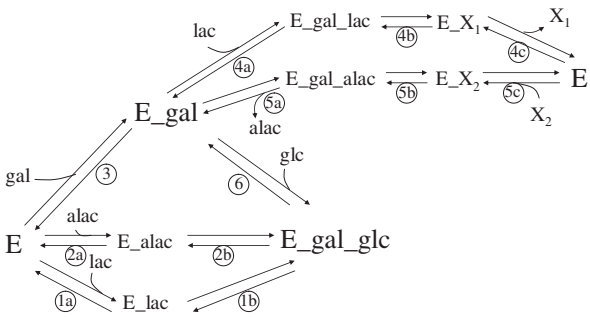

Fig. 10.3 The catalytic cycle of β-galactosidase

(*E_gal_glc*). According to the literature data (Huber et al. 1984, Huber et al. 1976), the process of glucose (*glc*) and galactose (*gal*) dissociation occurs in sequence (Stages 6, 3), via an intermediate enzyme form bound with galactose (*E_gal*). It follows from the scheme that the processes of lactose and allolactose hydrolysis are described by stages 1a-1b-6-3 and 2a-2b-6-3, and the transgalactosidase reaction proceeds through stages 1a-1b-2b-2a.

The reactions of galactosilation of lactose (4a-4b-4c) and allolactose (5a-5b-5c) are shown to be the main reactions of oligosaccharide formation in *E. coli* (Reeves and Sols 1973). We propose that, by analogy with glucose galactosilation (stages 6-1b-1a), these processes are realized through binding of lactose (stage 4a) or allolactose (stage 5a) to the enzyme form *E_gal* with the formation of trisaccharides *X1* and *X2* (specifying two types of trisaccharides: $gal+lac = X1,\ gal+alac = X2$).

10.3.2.2 Derivation of the Rate Equation of β-galactosidase

To simplify derivation and analysis of the equation for the rate of *beta-galactosidase* functioning, each process of trisaccharide formation (4a-4b-4c and 5a-5b-5c) was described by a single integral stage, neglecting intermediate enzyme forms (Fig. 10.4). It was an enforced approximation, because at present rather little is known about rate constants of these elementary stages, and the lack of kinetic data prevented us from assessing the contribution of each of them.

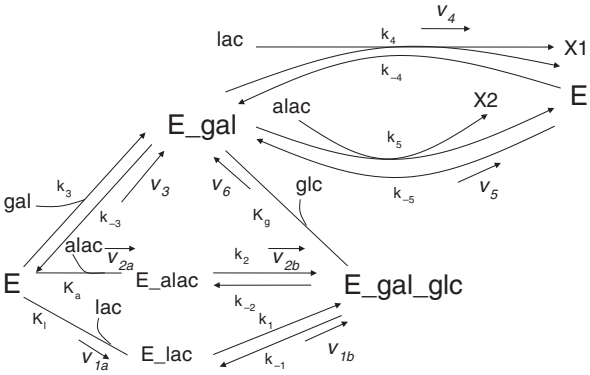

Fig. 10.4 The reduced catalytic cycle of β-galactosidase used for derivation of the rate equation

The simplified scheme of the catalytic cycle for the enzyme is given in Fig. 10.4. The corresponding rate as well as the rate or dissociation constant is indicated near each arrow.

With approximation of quasi stationary concentrations (Cornish-Bowden 2001), and entering a condition of the stationary for all the forms of the enzyme, the following system of equations was obtained

$$\begin{cases} (E\_lac)' = v_{1a} - v_{1b} = 0, \\ (E\_alac)' = v_{2a} - v_{2b} = 0, \\ (E\_gal\_glc)' = v_{1b} + v_{2b} - v_6 = 0, \\ (E)' = v_4 + v_5 - v_{1a} - v_{2a} - v_3 = 0, \\ (E\_gal)' = v_3 + v_6 - v_4 - v_5 = 0, \end{cases} \tag{10.5}$$

where dash is a complete time derivative. Solving this system with respect to the rate of reactions, we found that in a stationary (steady) state the rates of separate stages of catalytic cycle correlate with each other as follows:

$$\begin{cases} v_{1a} = v_{1b}, \\ v_{2a} = v_{2b}, \\ v_6 = v_{1b} + v_{2b}, \\ v_3 = -v_{1b} - v_{2b} + v_4 + v_5. \end{cases} \tag{10.6}$$

Thus, it turned out that all rates of elementary stages can be expressed via four velocities v_{1b}, v_{2b}, v_4 и v_5, hereinafter called «independent».

To derive the equation of the velocity of β-galactosidase, we formulated the velocities for the elementary stages of the catalytic cycle using mass action law assumption (Kotlarz and Buc 1977).

$$\begin{cases} v_{1b} = k_1 \cdot E\_lac - k_{-1} \cdot E\_gal\_glc, \\ v_{2b} = k_2 \cdot E\_alac - k_{-2} \cdot E\_gal\_glc, \\ v_3 = k_3 \cdot E \cdot gal - k_{-3} \cdot E\_gal, \\ v_4 = k_4 \cdot E\_gal \cdot lac - k_{-4} \cdot E \cdot X_1, \\ v_5 = k_5 \cdot E\_gal \cdot alac - k_{-5} \cdot E \cdot X_2. \end{cases} \tag{10.7}$$

The expressions of the velocities (10.7) were substituted into the fourth equation of the system (10.6) and the following equation was obtained:

$$\begin{aligned} &k_3 \cdot gal \cdot E + k_1 \cdot E\_lac + k_2 \cdot E\_alac + k_{-4} \cdot X_1 \cdot E + k_{-5} \cdot X_2 \cdot E - \\ &- k_{-3} \cdot E\_gal - k_{-1} \cdot E\_gal\_glc - k_{-2} \cdot E\_gal\_glc - \\ &- k_4 \cdot lac \cdot E\_gal - k_5 \cdot alac \cdot E\_gal = 0. \end{aligned} \tag{10.8}$$

We also accounted for the law of mass conservation for the total enzyme concentration:

$$E - E\_lac - E\_alac - E\_gal\_glc - E\_gal = E_0. \tag{10.9}$$

According to (Huber et al. 1984) the velocities of binding of lactose, allolactose and glucose are well above the rates of catalysis. So, we used approximation of fast equilibrium for stages 1a, 2a and 6. This allowed us, using the ratio of the constants of equilibrium for all quasi equilibrium stages, to express concentrations of different forms of the enzyme as concentrations of free form of the enzyme E and the complex of the enzyme and galactose E_gal:

$$\begin{aligned} E\_lac &= \frac{E \cdot lac}{K_l}, \\ E\_alac &= \frac{E \cdot alac}{K_a}, \\ E\_gal\_glc &= \frac{E\_gal \cdot glc}{K_g}. \end{aligned} \tag{10.10}$$

Substitution of the expression (10.10) in the formulae (10.8, 10.9) gives a system of two linear equation with respect to E и E_gal

$$\begin{cases} E\left(1 + \dfrac{lac}{K_l} + \dfrac{alac}{K_a}\right) + E\_gal\left(1 + \dfrac{glc}{K_g}\right) = E_0, \\ E\left(k_3 gal + k_1 \dfrac{lac}{K_l} + k_2 \dfrac{alac}{K_a} + k_{-4} X_1 + k_{-5} X_2\right) - \\ -E\_gal\left(k_{-3} + k_{-1} \dfrac{glc}{K_g} + k_{-2} \dfrac{glc}{K_g} + k_4 lac + k_5 alac\right) = 0. \end{cases}$$

Solving the system, the expressions for stationary concentrations of the enzyme states E and E_gal were obtained

$$\begin{aligned} E &= \frac{E_0}{\Delta}\left\{k_{-3} + \frac{glc}{K_g}(k_{-1} + k_{-2}) + k_4 lac + k_5 alac\right\}, \\ E\_gal &= \frac{E_0}{\Delta}\left\{k_3 gal + k_1 \frac{lac}{K_l} + k_2 \frac{alac}{K_a} + k_{-4} X_1 + k_{-5} X_2\right\}, \end{aligned} \tag{10.11}$$

where

$$\begin{aligned} \Delta = &\left\{k_3 + \frac{glc}{K_g}(k_{-1} + k_{-2}) + k_4 lac + k_5 alac\right\}\left(1 + \frac{lac}{K_l} + \frac{alac}{K_a}\right) + \\ &+ \left\{k_3 gal + k_1 \frac{lac}{K_l} + k_2 \frac{alac}{K_a} + k_{-4} X_1 + k_{-5} X_2\right\}\left(1 + \frac{glc}{K_g}\right). \end{aligned}$$

The concentrations of other stationary forms of the enzyme can be expressed using the formula (10.10). With knowledge of stationary concentrations of all the forms of the enzyme, it is possible to calculate the velocity of any elementary stage. Using (10.7, 10.10, and 10.11) we obtained the following

$$v_{1b} = \frac{E_0}{\Delta}\left\{k_1\frac{lac}{K_l}\left(k_{-3} + (k_{-1}+k_{-2})\frac{glc}{K_g} + k_4 lac + k_5 alac\right) - \right.$$
$$\left. - k_{-1}\frac{glc}{K_g}\left(k_3 gal + k_1\frac{lac}{K_l} + k_2\frac{alac}{K_a} + k_{-4}X_1 + k_{-5}X_2\right)\right\} \tag{10.12}$$

in much the same manner for other key velocities

$$v_{2b} = \frac{E_0}{\Delta}\left\{k_2\frac{alac}{K_a}\left(k_{-3} + (k_{-1}+k_{-2})\frac{glc}{K_g} + k_4 lac + k_5 alac\right) - \right.$$
$$\left. - k_{-2}\frac{glc}{K_g}\left(k_3 gal + k_1\frac{lac}{K_l} + k_2\frac{alac}{K_a} + k_{-4}X_1 + k_{-5}X_2\right)\right\} \tag{10.13}$$

$$v_4 = \frac{E_0}{\Delta}\left\{k_4 lac\left(k_3 gal + k_1\frac{lac}{K_l} + k_2\frac{alac}{K_a} + k_{-4}X_1 + k_{-5}X_2\right)\right.$$
$$\left. - k_{-4}X_1\left(k_{-3} + (k_{-1}+k_{-2})\frac{glc}{K_g} + k_4 lac + k_5 alac\right)\right\} \tag{10.14}$$

$$v_5 = \frac{E_0}{\Delta}\left\{k_5 alac\left(k_3 gal + k_1\frac{lac}{K_l} + k_2\frac{alac}{K_a} + k_{-4}X_1 + k_{-5}X_2\right)\right. \tag{10.15}$$
$$\left. - k_{-5}X_2\left(k_{-3} + (k_{-1}+k_{-2})\frac{glc}{K_g} + k_4 lac + k_5 alac\right)\right\}$$

The foregoing presents equations of the velocities for all the elementary stages. These expressions include the rate and dissociation constants. In order to describe the behavior of the real enzyme, the parameters of equations should be determined based on experimental data. In this case the experimental data were taken from (Burstein et al. 1965). The experiment was as follows. To a solution, containing 0.5 M of lactose, at zero point of time, β-galactosidase was added in such a way that its final concentration was equal to 130 μg per 1 ml. Concentration of lactose, allolactose, galactose, glucose and total concentration of oligosaccharides measured for 10 h have been measured parameters of the system.

Since the system described contains neither influxes nor effluxes of the matter, then in accordance with a kinetic profile depicted in Fig. 10.5 the change of

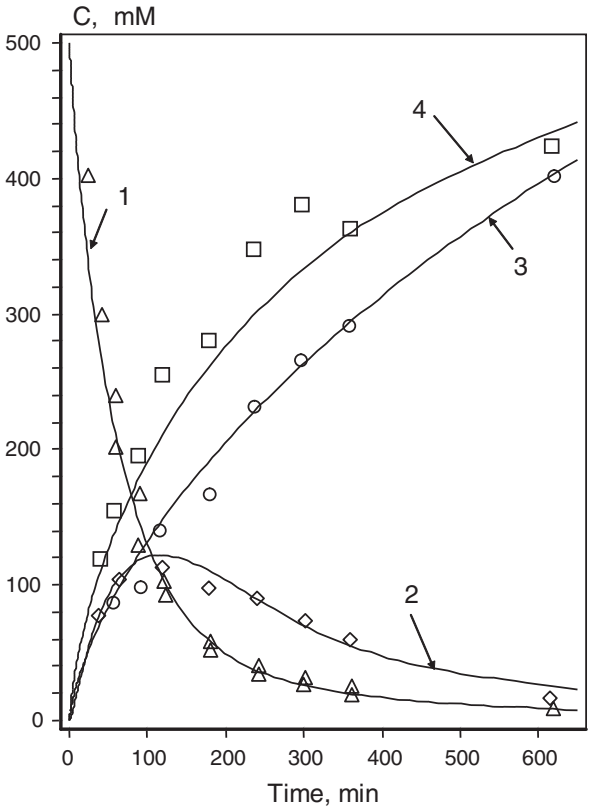

Fig. 10.5 β-galactosidase metabolites concentrations dependence on time described by the model and experimental data (Saier and Ramseier 1996): triangles (1-lactose concentration), rhombuses (2-allolactose concentration), circles (3-galactose concentration), squares (4-glucose concentration). Experimental conditions: 130 μg of *β-galactosidase* on 1 ml of the solution, T = 30 °C, $pH = 7.2$, $MgSO_4$ 6.7 mM, $NaCl$ 10 mM

concentrations of the metabolites in time is determined only by the activity of the enzyme and the following can be written

$$\begin{cases} (lac)' = -v_{1a} - v_4, \\ (alac)' = -v_{2a} - v_5, \\ (gal)' = -v_3, \\ (glc)' = -v_6, \\ (X_1)' = v_4, \\ (X_2)' = v_5. \end{cases} \tag{10.16}$$

In terms of the expression (10.6), which resulted from the approximation of quasistationary concentrations for all the forms of the enzyme, the system transforms into the following one

$$\begin{cases} (lac)' = -v_{1b} - v_4, \\ (alac)' = -v_{2b} - v_5, \\ (gal)' = -v_{1b} - v_{2b} - v_4 - v_5, \\ (glc)' = v_{1b} + v_{2b}, \\ (X_1)' = v_4, \\ (X_2)' = v_5. \end{cases} \tag{10.17}$$

The given system is a system of differential equations with concentrations of metabolites as variables. The system of Equations (10.18) represents two first linear integrals which correspond to the mass conservation laws for two monosaccharides-glucose and galactose:

$$\begin{aligned} glc + lac + alac + (X_1 + X_2) &= const_1, \\ gal + lac + alac + 2(X_1 + X_2) &= const_2. \end{aligned} \tag{10.18}$$

With the values of concentrations of metabolites in the system under study at zero point of time, it is possible to determine the values of the parameters $const_1$ и $const_2$. So, quantitative description of the above experiment reduces to a solution of Cauchy problem

$$\begin{cases} (lac)' = -v_1 - v_4, \\ (alac)' = -v_2 - v_5, \\ (X_1)' = v_4, \\ (X_2)' = v_5, \\ glc = 0,5M - lac - alac - (X_1 + X_2), \\ gal = 0,5M - lac - alac - 2(X_1 + X_2), \end{cases} \tag{10.19}$$

with initial terms

$$\begin{aligned} lac_0 &= 0,5M, \\ alac_0 = glc_0 = gal_0 = X_{10} = X_{20} &= 0M. \end{aligned}$$

10.3.2.3 Identification of the Parameters of β-galactosidase Rate Equation

In order for the model to describe the behavior of the real system it is necessary to identify the parameters included in the equation of the rate of an enzyme based on experimental data. In our work we used as a criterion of adequacy of the model constructed to the real enzyme a sum of quadratic deviations of theoretical values, the results of modelling from the experimental points from the work (Huber et al. 1976). In this connection a search of optimal values of the model parameters determined by the system of Equation (10.19) was in designating of such a set of constants, where the criterion should reach a minimum. Minimization of deviation was made according to the Hook-Jeeves technique within the wide range of possible values of the constants of rate and dissociation.

All the algorithms used for solving the system of differential equations and searching optimal values of the parameters were developed using the DBsolve software 7.01 (Gizzatkulov et al. 2004). The parameters identified for β-galactosidase are given in Table 10.2. Experimental estimates available for some constants are given in brackets. Figure 10.5 represents the results of fitting of experimental data with our developed model.

Table 10.2 β-galactosidase model parameters values estimated from experimental data published in (Huber et al. 1976)

Model parameter	Value	Model parameter	Value
k_1	$1,0 \cdot 10^4$ min^{-1}	k_{-1}	$0,8 \cdot 10^3$ min^{-1} $1,0 \cdot 10^4$ min^{-1}
k_2	$4 \cdot 10^4$ min^{-1}	k_{-2}	(2, 3 10^4 min^{-1} (Kurganov 1978))
k_3	$3 \cdot 10^1$ min^{-1} mM^{-1}	k_{-3}	$1,6 \cdot 10^4$ min^{-1}
k_4	$2 \cdot 10^1$ min^{-1} mM^{-1}	k_{-4}	$0,8 \cdot 10^3$ min^{-1} mM^{-1}
k_5	$2 \cdot 10^1$ min^{-1} mM^{-1}	k_{-5}	$0,8 \cdot 10^3$ min^{-1} mM^{-1}
K_l	0,7 mM (1,3 mM (Kotlarz and Buc 1977))	K_g	14 mM (17 mM (Kurganov 1978))
K_a	0,8 mM		

We used the model to study the ratio between different activities of an enzyme. β-galactosidase has several activities: formation of glucose and galactose, transformation of lactose into allolactose and synthesis of trisaccharides. Which of these activities are dominating and how does the contribution of each activity depend on the concentration of the substrates and products? The answers to these questions enable us to understand better how the functioning of an enzyme is controlled by the substrate. To solve this problem we used the equations of the rates at fixed zero values of the concentration of allolactose, galactose, glucose and trisaccharides and changing concentration of lactose within the range of 0–5 mM (Fig. 10.6). It is possible to interpret this study as an attempt to forecast theoretically the experimental

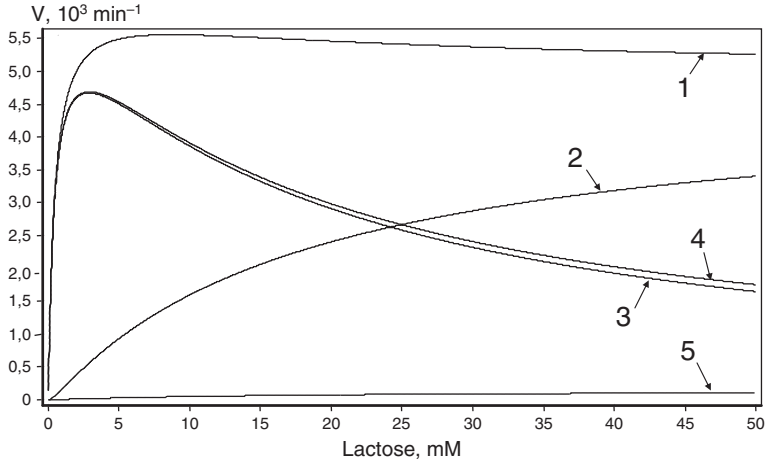

Fig. 10.6 The model fluxes distribution and their dependences on lactose concentration: 1- stationary rate of lactose consumption. 2,3,4,5-stationary synthesis rates of allolactose, galactose, glucose, and trisaccharides correspondingly. The model conditions: alac = oligo = 0 mM, glc = 0–1000 mM, gal = 0–1000 mM

data on measuring initial rates of lactose utilization and synthesis of various products depending on the concentration of the main substrate.

As seen from Fig. 10.6 the dependence of the rate of lactose consumption on the concentration of the latter in the conditions has clear deviation from the classical law of Michaelis-Menten, namely, at lactose concentrations higher than 10 mM a small decrease of the consumption rate is seen. The rates of the synthesis of glucose and galactose have a pronounced optima; at lactose concentration of 25 mM the yield is maximal. The rate of allolactose synthesis under the same conditions increases monotonically within the whole range studied. At a lactose concentration of 25 mM the rate of allolactose synthesis becomes equal to the rate of monosaccharides synthesis. It should be noted that the situation where the rate of allolactose synthesis can exceed the rate of monosaccharides formation *in vivo* is most probably impossible, since actual lactose concentration inside the bacterium is deliberately lower than the modeled one.

Within the whole range of lactose concentrations the outflow of the substance for the synthesis of byproducts (trisaccharides) turns out to be very low and does not exceed 3% of the rate of lactose consumption. We can conclude that under conditions close to the intracellular ones the substance outflow for the synthesis of trisaccharides can be ignored without any loss in exactness described.

Besides the data shown in Fig. 10.6 we studied how the permanent reaction rates depended on the concentrations of glucose and galactose (data are not available), since metabolites could be in higher concentrations in actual bacteria. It turned out that at concentrations up to 1 mM of each of the monosaccharides the values of the fixed rates remained unchanged. It is possible to explain this by the fact that equilibrium of lactose hydrolysis is significantly shifted towards higher values, hence decomposition is, in fact, irreversible in the range studied resulting in weak sensitivity of the enzyme to monosaccharides.

We constructed a kinetic model of *E. coli* β-galactosidase, and determined the parameters included in the rate expression. The model obtained enables us to describe not only experimental data used for identification of the parameters, but to predict the behavior of the enzyme for other conditions (for example *in vivo*). Besides we showed in the work that the model used can "simulate" another type of experiment, like measuring of initial rates at variable concentrations of one of the substrates.

10.3.3 Kinetic Model of the E. coli *Citrate Synthase*

Citrate Synthase (EC 2.3.3.1, *gltA*) is the key enzyme of the Krebs cycle – the central part of the cell's energy metabolism. It catalyzes the first step of carbon atoms entering to the cycle, i.e. acetyl coenzyme A (AcCoA) condensates with oxaloacetate (OAA) resulting in citrate (Cit) production and release of coenzyme A (CoA) (Neidhardt and Curtiss 1996): $\mathrm{AcCoA} + \mathrm{OAA} = \mathrm{Cit} + \mathrm{CoA}$. The enzyme has complex regulation by the key metabolites (ATP, NADH) which reflect energy state of the cell. That is why it is so imprtant to obtain realistic description of the enzyme as a

part of the whole model of *E. coli* central metabolism. To date there is no generally accepted opinion in literature about the mechanism of the *E. coli* citrate synthase reaction. There exists disagreement in assumptions about the mechanism of citrate synthase reaction: whether substrates binding to the enzyme is arbitrary (Wright and Sanwal 1971a) or ordered (Pereira et al. 1994). The order of substrates binding is also disputed. In our model we have assumed AcCoA being the first substrate according to ATP inhibition studies (Jangaard et al. 1968a). Citrate synthase is known to have a complex regulatory pattern – the activity of the enzyme is pH-dependent and is modulated by inhibitors – ATP, NADH, 2-ketoglutarate. We have accounted for these regulators in our developed catalytic cycle for citrate synthase. We have derived the rate equation, and estimated the enzyme's kinetic parameters. Their values have been verified using an independent set of experimental data published in (Jangaard et al. 1968a). The enzyme's concentrations in *E. coli* cells grown under aerobic conditions on acetate and glucose have been estimated from *E. coli* cell extracts' specific activities.

When constructing the model we have used the following facts about *E. coli* citrate synthase functioning, known from literature:

1. Citrate synthase of gram-negative bacteria is a hexamer. Sigmoid dependence of initial rate on AcCoA was obtained under zero concentration of KCl in (Pereira et al. 1994). The effect was not observed under 0.1 M KCl addition (Pereira et al. 1994). As the concentration of 0.1 M KCl is physiological for *E. coli* we have not described the sigmoid dependence observed under KCl = 0.
2. The reaction is practically irreversible with an equilibrium constant of $2.24^{*}10^{6}$ (Guynn et al. 1973).
3. NADH and a-ketoglutarate are citrate synthase's inhibitors noncompetitive to oxaloacetate (Jangaard et al. 1968a).
4. ATP is the inhibitor competitive in respect to AcCoA and noncompetitive to oxaloacetate (Jangaard et al. 1968a).
5. The enzyme's maximal activity depends on pH without inhibitors and with ATP addition (Jangaard et al. 1968a). It was shown that ATP moves the maximum of the bell-shaped pH-dependence to the right and decreases the rate in its maximum (Jangaard et al. 1968a).
6. *E. coli* Citrate synthase kinetic parameters known from literature:

$$
\begin{aligned}
K_m^{AcCoA} &= 0.11 \text{ mM (Faloona and Srere 1969a);} \\
K_m^{OAA} &= 0.021 \text{ (pH 8.1, t } = 21^{\circ}\text{C in the presence of 0.1M KCl)} \\
&\quad \text{(Faloona and Srere 1969a);} \\
K_d^{AcCoA} &= 0.7 \text{ mM (pH 8.0) (Faloona and Srere 1969b);} \\
k_{cat} &= 4860 1/\text{ min (pH 8.0) (Donald et al. 1991);} \\
pH_{opt} &= 7.3 \text{(Jangaard et al. 1968a).}
\end{aligned}
\tag{10.20}
$$

10.3.3.1 Construction of Citrate Synthase Catalytic Cycle

As there is disagreement about citrate synthase's mechanism we have used experimental data on the enzyme inhibition by ATP. ATP was shown to be a competitive inhibitor with respect to AcCoA and noncompetitive to oxaloacetate (Jangaard et al. 1968a). This can be observed only when AcCoA is the first substrate. So we have assumed that citrate synthase functions according to Irreversible Ordered Bi Bi mechanism by Cleland classification (Cleland 1963), with AcCoA binding first. The scheme of this catalytic cycle is presented in Fig. 10.7. We also have taken into account inhibitors α-ketoglutarate and NADH which bind to two enzyme forms – enzyme bound with AcCoA, and enzyme bound with AcCoA and OAA (Fig. 10.7). This assumption allowed us to describe experimental data on enzyme inhibition. ATP binding to free enzyme form was also included into the scheme (Fig. 10.7). Moreover we have described dependence of the enzyme activity on pH (pH-dependence). The classic assumption (Cornish-Bowden 2001) was applied that enzyme can be protonated in its active site and the singly protonated form is active whereas non protonated and doubly protonated forms are inactive (Fig. 10.7). To describe ATP effects on pH-dependence (see clause 5) we have assumed that the active form is ATP bound to doubly protonated enzyme as only in this case the maximum could decrease and its shift to the higher values of proton concentration could be observed.

10.3.3.2 Derivation of Citrate Synthase Rate Equation

Derivation of Rate Equation in Terms of Catalytic Cycle Parameters

As the reaction is almost irreversible (Guynn et al. 1973) we have described the enzyme working only in a forward direction in respect of rate dependence on substrates and effectors concentrations. On the scheme (Fig. 10.7) the stages of substrates binding are shown as reversible and the stage of product formation is irreversible with rate constant k_3. The rate equation has been derived based on the assumption that stages of effector and proton binding are much faster than the catalytic stage

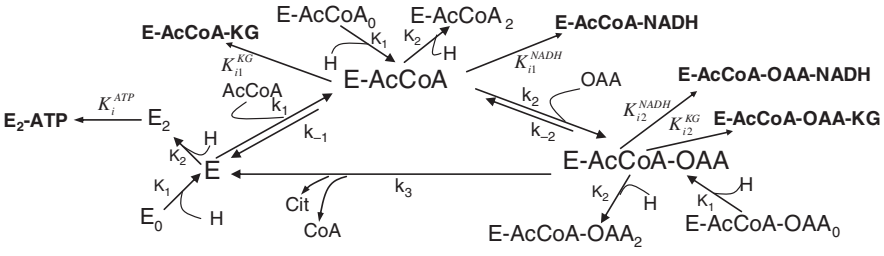

Fig. 10.7 The scheme of *E. coli* citrate synthase catalytic cycle. Designations: E – Citrate Synthase; E_0, E-AcCoA$_0$, E-AcCoA-OAA$_0$ – deprotonated enzyme forms; E, E-AcCoA, E-AcCoA-OAA – once protonated enzyme forms; E_2, E-AcCoA$_2$, E-AcCoA-OAA$_2$ – twice protonated enzyme forms

and the stages of substrates binding. The stages of protons binding were characterized by two parameters: dissociation constants for proton dissociation from doubly and singly protonated enzyme forms. With these assumptions we have derived the following rate equation for citrate synthase:

$$V = CS\frac{k_1k_2k_3 \cdot AcCoA \cdot OAA}{(k_{-1}k_3 + k_{-1}k_{-2} + k_2k_3 \cdot OAA)\left(1 + \frac{K_{d1}^H}{H} + \frac{H}{K_{d2}^H}\left(1 + \frac{ATP}{K_i^{ATP}}\right)\right) + \\ + AcCoA(k_1k_3 + k_1k_{-2})\left(1 + \frac{K_{d1}^H}{H} + \frac{H}{K_{d2}^H} + \frac{KG}{K_{i1}^{KG}} + \frac{NADH}{K_{i1}^{NADH}}\right) + \\ + k_1k_2 \cdot AcCoA \cdot OAA\left(1 + \frac{K_{d1}^H}{H} + \frac{H}{K_{d2}^H} + \frac{KG}{K_{i2}^{KG}} + \frac{NADH}{K_{i2}^{NADH}}\right) \tag{10.21}$$

Here $k_{1,-1}$, $k_{2,-2}$, k_3 are rate constants for corresponding stages of the catalytic cycle, CS is the enzyme concentration, K_{d1}^H, K_{d2}^H, K_i^{ATP}, K_{i1}^{KG}, K_{i2}^{KG}, K_{i1}^{NADH}, K_{i2}^{NADH} are dissociation constants for corresponding inhibitors and protons.

Derivation of Rate Expression in Terms of Kinetic Parameters (Michaelis Constants, Inhibition Constants, Catalytic Constants etc.)

To express rate equation (10.21) in terms of experimentally measured kinetic parameters we have found their expressions from Equation (10.21):

$$V_{\max} = CS\frac{k_3}{\left(1 + \frac{K_{d1}^H}{H} + \frac{H}{K_{d2}^H}\right)}; K_m^{AcCoA} = \frac{k_3}{k_1}; K_m^{OAA} = \frac{k_3 + k_{-2}}{k_2} \tag{10.22}$$

Using these expressions (10.22) we could rewrite rate equation in the following form:

$$V = CS\frac{k_{cat0} \cdot AcCoA \cdot OAA}{(K_d^{AcCoA} \cdot K_m^{OAA} + K_m^{AcCoA} \cdot OAA)\left(1 + \frac{K_{d1}^H}{H} + \frac{H}{K_{d2}^H}\left(1 + \frac{ATP}{K_i^{ATP}}\right)\right) + \\ + AcCoA \cdot K_m^{OAA} \cdot \left(1 + \frac{K_{d1}^H}{H} + \frac{H}{K_{d2}^H} + \frac{KG}{K_{i1}^{KG}} + \frac{NADH}{K_{i1}^{NADH}}\right) + \\ + AcCoA \cdot OAA \cdot \left(1 + \frac{K_{d1}^H}{H} + \frac{H}{K_{d2}^H} + \frac{KG}{K_{i2}^{KG}} + \frac{NADH}{K_{i2}^{NADH}}\right) \tag{10.23}$$

here,

$$k_{cat0} = k_3; K_d^{AcCoA} = \frac{k_{-1}}{k_1}$$

10.3.3.3 Estimation of the Citrate Synthase Kinetic Parameters

There were 12 parameters in rate equation (10.23): three of them were known from literature, 8 parameters have been estimated from *in vitro* experimental data whereas enzyme concentration in *E. coli* cells could not be found from *in vitro* data and was estimated from *E. coli* cell extract specific activity. As the catalytic constant of the enzyme was estimated in literature under fixed pH value conditions (k_{cat} = 4860 1/ min, pH 8.0 (Donald et al. 1991)), we have used it for parameter k_{cat0} determination: $k_{cat0} = k_{cat}\left(1 + \frac{K_{d1}^H}{H} + \frac{H}{K_{d2}^H}\right)$. So we have reduced the number of unknown parameters to 7. Further, we have determined some of the parameters from experimental data obtained in the absence of inhibitors. We have used initial rate dependencies on substrate AcCoA from two sources (Faloona and Srere 1969b, Wright and Sanwal 1971b): five curves with different concentrations of oxaloacetate (Fig. 10.8a,b), two initial rate dependencies on oxaloacetate with fixed concentration of AcCoA (Faloona and Srere 1969b) (Fig. 10.8c), and pH-dependence (Jangaard et al. 1968b) (Fig. 10.8d). We have found such a set of parameters which allowed us to describe all these data with a rate equation (10.23). Fitting results are presented on Fig. 10.8 Here is the list of parameter values:

$$K_{d1}^H = 1e-5\,mM; K_{d2}^H = 2e-4\,mM; K_m^{AcCoA} = 0.18\,mM;$$
$$K_m^{OAA} = 0.04\,mM; K_d^{AcCoA} = 0.1\,mM; K_i^{ATP} = 0.58\,mM$$

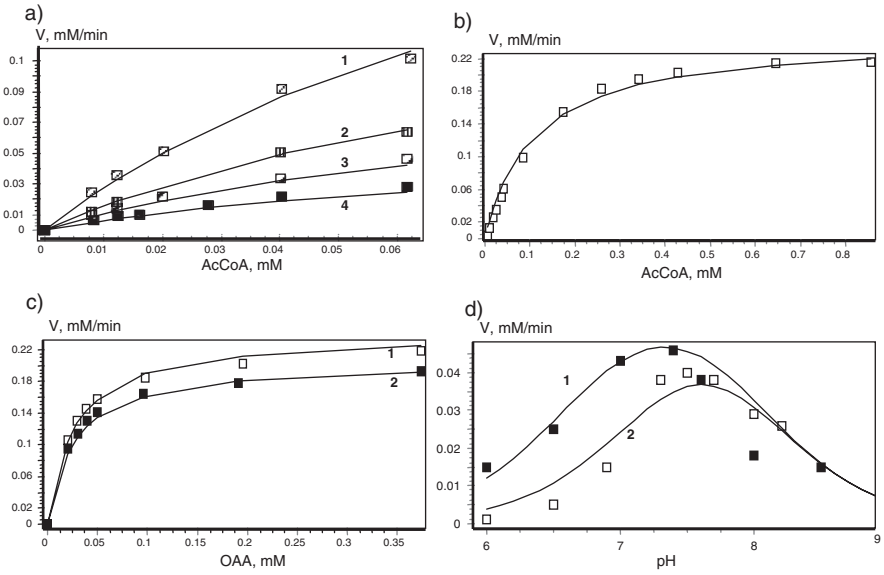

Fig. 10.8 Citrate synthase initial rate dependence on substrates concentrations and pH described by experimental points and rate equation (10.23): (**a**) OAA concentration: 1–0.1; 2–0.02; 3–0.005; 4–0.01 mM (Ivanitsky et al. 1978); (**b**) OAA concentration was 0.5 mM (Ivanitsky et al. 1978); (**c**) AcCoA concentration: 1–0.5; 2–0.25 mM (Ewings and Doelle 1980); (**d**) AcCoA = 0.05 mM; OAA = 0.1 mM; ATP concentration: 1–0; 2–2 mM (Cleland 1963)

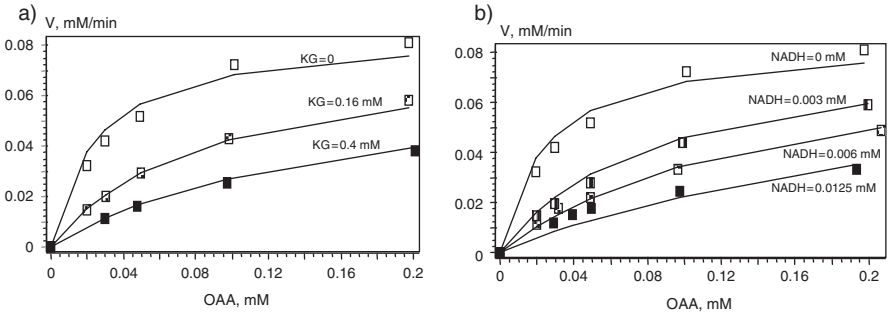

Fig. 10.9 Citrate synthase initial rate dependence on concentrations of substrates in the presence of inhibitors described by experimental points and rate equation (10.23)

To estimate the inhibition constants we have used experimental data on initial reaction rate dependence on substrates concentrations in the presence of different concentrations of the inhibitors α-ketoglutarate and NADH (Wright and Sanwal 1971b):

$$K_{i1}^{KG} = 0.015 \text{ mM}; K_{i2}^{KG} = 0.256 \text{ mM}; K_{i1}^{NADH} = 3.3e-4 \text{ mM};$$
$$K_{i2}^{NADH} = 8.4e-3 \text{ mM}.$$

The results of fitting are shown on Fig. 10.9.

On the next stage we have verified our model of citrate synthase functioning on experimental data which were not used for fitting. We have used the data on initial rate dependence on substrates concentration in the presence of ATP (Jangaard et al. 1968b). It was shown that the rate equation (10.23) and estimated parameters values allowed us to describe the independent set of experimental curves (Fig. 10.10).

Estimation of citrate synthase concentration depending on *E. coli* growth conditions

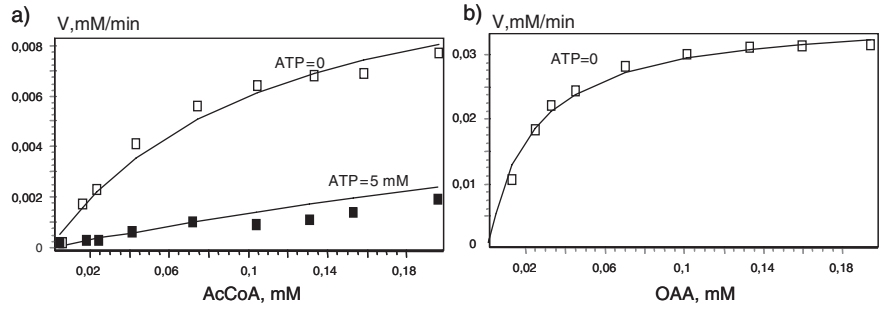

Fig. 10.10 Model verification. Citrate synthase initial rate dependence on concentrations of substrates described by experimental points (Cleland 1963) and rate equation (10.23)

Specific citrate synthase activity (SA) of *E. coli* cells extract grown on acetate has been measured in (Cornish-Bowden 2001):

$$\mathrm{SA} = 0.25 \text{ micromoles/min}^{*} \text{ mg}_{\text{extract protein}}$$

Assuming that 1 mg of *E. coli* cells protein corresponds to 5.5 microL of intracellular volume (Jangaard et al. 1968b) we have calculated the enzyme's maximal rate from the specific activity: $\mathrm{V_{max}} = 45.5\,\mathrm{mM/\,min}$. Further citrate synthase concentration can be calculated by dividing of maximal rate by catalytic constant of the enzyme. In this case, however, we should use the value of catalytic constant obtained at the same pH as the maximal velocity value, i.e. at physiological pH of 7.3 (Padan et al. 1981). We have calculated the required value of the catalytic constant in accordance with the obtained pH-dependence of the enzyme:

$$k_{cat}^{pH7.3} = \frac{k_{cat0}}{\left(1 + \frac{K_{d1}^{H}}{H} + \frac{H}{K_{d2}^{H}}\right)} = \frac{9941}{\left(1 + \frac{1e-5}{1e-4.3} + \frac{1e-4.3}{2.2e-4}\right)} = 6966\ (1/\,\mathrm{min})$$

So we could calculate citrate synthase concentration in *E. coli* grown aerobically on acetate:

$$CS_{acetate} = V_{\max}^{acetate} / k_{cat}^{pH7.3} = 6.5\ (microM)$$

In the same way we have calculated the enzyme concentration which should be observed in *E. coli* cell grown aerobically on glucose. We have used citrate synthase specific activity measured on the extract of *E. coli* cells grown on glucose:

$\mathrm{SA} = 0{,}05 \text{ micromoles/min}^{*}\mathrm{mg}_{\text{extract protein}}$ (Peng and Shimizu 2003).

Maximal velocity has been calculated as $\mathrm{V_{max}} = 9\,\mathrm{mM/\,min}$, and citrate synthase concentration in the cell in these conditions was estimated:

$$CS_{glucose} = V_{\max}^{glucose} / k_{cat}^{pH7.3} = 1.3\ (microM)$$

So we have constructed a kinetic model of *E. coli* citrate synthase functioning – the rate equation has been derived and kinetic parameters have been estimated. We have taken into account known inhibitory effects and pH dependence of the enzyme activity. This allowed us to describe a set of experimental data obtained under different pH values. Plausibility of the model was confirmed by its ability to describe an independent data set (Jangaard et al. 1968b) which had not been used for model parameters determination. Citrate synthase concentrations in *E. coli* cells grown aerobically on acetate and glucose have been obtained.

10.4 Conclusion

We have illustrated our kinetic modeling approach using three *E. coli* enzymes. We propose that only a detailed description of individual enzymes allows realistic kinetic models of the whole pathways in the cell to be obtained. The ultimate goal is to integrate all available *in vitro* experimental data in the description of the enzyme. First, we use relevant data to reconstruct the enzyme's catalytic cycle. Then we derive the rate equation of the enzyme. The next and most complicated step is to define such values of kinetic parameters from the rate equation that would allow us to describe all experimental dependencies measured *in vitro*. Here we have illustrated our strategy with three non-trivial and rather complicated enzyme models: allosteric tetramer phosphofructokinase-1, citrate synthase with its regulation by ATP and pH, and β-galactosidase validated against time dependencies of its substrates.

Analysis of the phosphofruktokinase-1 model allowed us to predict new operational properties of phosphofructokinase-1, such as cooperative action of allosteric effectors (PEP, ADP and GDP), competitive inhibition by free form of ATP and influence of magnesium ions on the enzyme rate.

We used the modelling to study the ratio between different activities of β-galactosidase. It turned out, that at lactose concentration of 25 mM the rate of allolactose synthesis becomes equal to the rate of monosaccharides synthesis. Within the whole range of lactose concentrations the outflow of the substance for the synthesis of trisaccharides does not exceed 3% of the lactose consumption. We also found that concentrations of glucose and galactose up to 1 mM did not change the consumption and production rates.

The kinetic model of *E. coli* citrate synthase allowed us to get insight into some important regulatory features of the enzyme catalytic mechanism. According to ATP inhibition studies (Jangaard et al. 1968b) we have proposed Ordered Bi Bi citrate synthase's mechanism with AcCoA binding first. Inhibition experimental data allowed us to accept the hypothesis that the inhibitors alpha-ketoglutarate and NADH binds to two enzyme forms (the enzyme bound with AcCoA and with both AcCoA and OAA). To describe ATP effects on pH-dependence (Jangaard et al. 1968b) we have assumed that the active enzyme form corresponds to the complex of twice protonated enzyme with ATP. With the use of our model we managed to estimate the concentration of citrate synthase in *E. coli* cells grown aerobically on acetate and glucose.

The models we presented in this paper prove that developing of detailed enzyme kinetic models can be essential to capture the enzyme regulatory properties. We illustrated how the detailed kinetic model of the enzyme can be further reduced to derive a reaction rate equation which inherits key regulatory effects included in the original detailed description, and allows to consistently approximate large sets of *in vitro* experimental data. Individual reaction rates derived in such a way can be further integrated into higher level kinetic models of *E. coli* metabolic pathways. Pathway models will in their turn allow investigating higher level regulatory effects in bacterial metabolic networks, observed in cellular extracts and *in vivo*. We hope that the kinetic modeling approach in general, and three kinetic models of *E. coli*

enzymes in particular, will be useful for future whole cell models of *E. coli*, and practical applications in metabolic engineering and synthetic biology.

Acknowledgments For support of this work we acknowledge GlaxoSmithKline, Institute for Systems Biology Sankt Petersburg, EU FP6 EC-MOAN and Centre for Systems Biology at Edinburgh (CSBE). CSBE is a Centre for Integrative Systems Biology supported by BBSRC and EPSRC.

Abbreviations

PfkA	Phosphofructokinase-1
F6P	fructose-6-phosphate
F16bP	fructose-1,6-biphosphate
PEP	phosphoenolpyruvate
$ATPMg^{2-}$	magnesium form of ATP
lac	lactose
alac	allolactose
glc	glucose
gal	galactose
oligo	oligosaccharides
E_gal, E_lac, E_alac	β-galactosidase enzyme form bound with galactose, lactose, allolactose
E_gal_glc	ternary complex of β-galactosidase enzyme form bound with galactose and glucose
gltA	Citrate Synthase
CS	Citrate synthase concentration
AcCoA	acetyl coenzyme A
OAA	oxaloacetate
Cit	citrate
CoA	coenzyme A
KG	2-ketoglutarate
H	proton
SA	specific activity of the enzyme

References

Ausat I, Le Bras G, Garel J-R (1997) Allosteric Activation Increases the Maximum Velocity of *E. coli* Phosphofructokinase. J Mol Biol 267:476–80

Babul J (1978) Phosphofructokinases from *Escherichia coli*. Purification and characterization of the nonallosteric isozyme. J Biol Chem 253(12):4350–5

Barrett CL, Kim TY, Kim HU et al. (2006) Systems biology as a foundation for genome-scale synthetic biology. Curr Opin Biotechnol 17(5):488–92

Berger SA, Evans PR (1991) Steady-state fluorescence of *Escherichia coli* phosphofructokinase reveals a regulatory role for ATP. Biochemistry 30(34):8477–80

Blangy D, Buc H, Monod J (1968) Kinetics of the allosteric interactions of phosphofructokinase from *Escherichia coli*. J Mol Biol 31(1):13–35

Burstein C, Cohn M, Kepes A et al. (1965) [Role of Lactose and Its Metabolic Products in the Induction of the Lactose Operon in *Escherichia Coli*.]. Biochim Biophys Acta 95:634–9

Campos G, Guixe V, Babul J (1984) Kinetic mechanism of phosphofructokinase-2 from *Escherichia coli*. A mutant enzyme with a different mechanism. J Biol Chem 259(10):6147–52

Cleland WW (1963) The kinetics of enzyme-catalyzed reactions with two or more substrates or products. I. Nomenclature and rate equations. Biochim Biophys Acta 67:104–37

Cornish-Bowden A (2001) Fundamentals of Enzyme kinetics. London

Demin O, Goryanin I (2008) Kinetic modelling in systems biology. Chapman & Hall/CRC, Virginia Beach, VA

Demin OV, Goryanin, II, Dronov S et al. (2004) Kinetic model of imidazologlycerol-phosphate synthetase from *Escherichia coli*. Biochemistry (Mosc) 69(12):1324–35

Deville-Bonne D, Bourgain F, Garel JR (1991a) pH dependence of the kinetic properties of allosteric phosphofructokinase from *Escherichia coli*. Biochemistry 30(23):5750–4

Deville-Bonne D, Laine R, Garel JR (1991b) Substrate antagonism in the kinetic mechanism of *E. coli* phosphofructokinase-1. FEBS Lett 290(1–2):173–6

Donald LJ, Crane BR, Anderson DH et al. (1991) The role of cysteine 206 in allosteric inhibition of *Escherichia coli* citrate synthase. Studies by chemical modification, site-directed mutagenesis, and 19F NMR. J Biol Chem 266(31):20709–13

Edwards JS, Ibarra RU, Palsson BO (2001) *In silico* predictions of *Escherichia coli* metabolic capabilities are consistent with experimental data. Nat Biotechnol 19(2):125–30

Endy D (2005) Foundations for engineering biology. Nature 438(7067):449–53

Ewings KN, Doelle HW (1980) Further kinetic characterization of the non-allosteric phosphofructokinase from *Escherichia coli* K-12. Biochim Biophys Acta 615(1):103–12

Faloona GR, Srere PA (1969a) *Escherichbia coli* citrate synthase. Purification and the effect of potassium on some properties. Biochemistry 8:4497–503

Faloona GR, Srere PA (1969b) *Escherichia coli* citrate synthase. Purification and the effect of potassium on some properties. Biochemistry 8(11):4497–503

Feist AM, Henry CS, Reed JL et al. (2007) A genome-scale metabolic reconstruction for *Escherichia coli* K-12 MG1655 that accounts for 1260 ORFs and thermodynamic information. Mol Syst Biol 3:121

Gizzatkulov N, Klimov A, Lebedeva G, Demin O (2004) DBSolve7: New update version to develop and analyse models of complex biological systems. 12th International Conference on Intelligent Systems for Molecular Biology: 210

Guixe V, Babul J (1985) Effect of ATP on phosphofructokinase-2 from *Escherichia coli*. A mutant enzyme altered in the allosteric site for MgATP. J Biol Chem 260(20):11001–5

Guynn RW, Gelberg HJ, Veech RL (1973) Equilibrium Constants of the Malate Dehydrogenase, Citrate Synthase, Citrate Lyase, and Acetyl Coenzyme A Hydrolysis Reactions under Physiological Conditions. J Biol Chem 248:6957–65

Han MJ, Lee SY (2006) The *Escherichia coli* proteome: past, present, and future prospects. Microbiol Mol Biol Rev 70(2):362–439

Huber RE, Gaunt MT, Hurlburt KL (1984) Binding and reactivity at the "glucose" site of galactosyl-beta-galactosidase (*Escherichia coli*). Arch Biochem Biophysics 234:151–60

Huber RE, Kurz G, Wallenfels K (1976) A quantitation of the factors which affect the hydrolase and transgalactosylase activities of beta-galactosidase (*E. coli*) on lactose. Biochemistry 15:1994–2001

Ishii N, Nakahigashi K, Baba T et al. (2007) Multiple high-throughput analyses monitor the response of *E. coli* to perturbations. Science 316:593–7

Ishii N, Nakahigashi K, Baba T et al. (2007) Multiple high-throughput analyses monitor the response of *E. coli* to perturbations. Science 316(5824):593–7

Ivanitsky GR, Krinsky V, Selkov EE (1978) Mathematical biophysics of the cell. Nauka, Moscow

Jangaard NO, Unkeless J, Atkinson DE (1968a) The inhibition of Citrate Synthase by adenosine triphosphate. Biochim Biophys Acta 151:225–35

Jangaard NO, Unkeless J, Atkinson DE (1968b) The inhibition of citrate synthase by adenosine triphosphate. Biochim Biophys Acta 151(1):225–35

Jobe A, Bourgeois S (1972) lac Repressor-operator interaction. VI. The natural inducer of the *lac* operon. J Mol Biol 69(3):397–408

Kim HU, Kim TY, Lee SY (2008) Metabolic flux analysis and metabolic engineering of microorganisms. Mol Biosyst 4(2):113–20

Kotlarz D, Buc H (1977) Two *Escherichia coli* fructose-6-phosphate kinases. Preparative purification, oligomeric structure and immunological studies. Biochim Biophys Acta 484(1): 35–48

Kotlarz D, Buc H (1982) Phosphofructokinases from *Escherichia coli*. Methods Enzymol 90 Pt E:60–70

Kurganov BI (1978) Allosteric enzymes. Moscow

Lee JM, Gianchandani EP, Papin JA (2006) Flux balance analysis in the era of metabolomics. Brief Bioinform 7(2):140–50

Lee KH, Park JH, Kim TY et al. (2007) Systems metabolic engineering of *Escherichia coli* for L-threonine production. Mol Syst Biol 3:149

Lee SJ, Lee DY, Kim TY et al. (2005) Metabolic engineering of *Escherichia coli* for enhanced production of succinic acid, based on genome comparison and *in silico* gene knockout simulation. Appl Environ Microbiol 71(12):7880–7

Monod J, Wyman J, Changeux JP (1965) On the Nature of Allosteric Transitions: a Plausible Model. J Mol Biol 12:88–118

Neidhardt FC, Curtiss R (1996) *Escherichia coli* and *Salmonella*: cellular and molecular biology. ASM Press, Washington, DC

Padan E, Zilberstein D, Schuldiner S (1981) pH homeostasis in bacteria. Biochim Biophys Acta 650(2–3):151–66

Park JH, Lee KH, Kim TY et al. (2007) Metabolic engineering of *Escherichia coli* for the production of L-valine based on transcriptome analysis and *in silico* gene knockout simulation. Proc Natl Acad Sci USA 104(19):7797–802

Peng L, Shimizu K (2003) Global metabolic regulation analysis for *Escherichia coli* K12 based on protein expression by 2-dimensional electrophoresis and enzyme activity measurement. Appl Microbiol Biotechnol 61(2):163–78

Pereira DS, Donald LJ, Hosfield DJ et al. (1994) Active site mutants of *Escherichia coli* citrate synthase. Effects of mutations on catalytic and allosteric properties. J Biol Chem 269:412–7

Perna NT, Plunkett G 3rd, Burland V et al. (2001) Genome sequence of enterohaemorrhagic *Escherichia coli* O157:H7. Nature 409:529–33

Price N, Reed J, Palsson B (2004) Genome-scale models of microbial cells: evaluating the consequences of constraints. Nat Rev Microbiol 2:886–97

Reeves RE, Sols A (1973) Regulation of *Escherichia coli* phosphofructokinase in situ. Biochem Biophys Res Commun 50(2):459–66

Rye S, Ramseier TM, Michotey V et al. (1995) Effect of the FruR regulator on transcription of *pts* operon in *Escherichia coli*. J Biol Chem 270:2489–96

Saier MH, Jr., Ramseier TM (1996) The catabolite repressor/activator (*Cra*) protein of enteric bacteria. J Bacteriol 178(12):3411–7

Saier MH Jr, Crasnier M (1996) Inducer exclusion and the regulation of sugar transport. Res Microbiol 147:482–9

Schütz R, Küpfer L, Sauer U (2007) Systematic evaluation of objective functions for predicting intracellular fluxes in *E. coli*. Mol Sys Biol 3:119

Selkov E, Basmanova S, Gaasterland T et al. (1996) The metabolic pathway collection from EMP: the enzymes and metabolic pathways database. Nucleic Acids Res 24(1):26–8

Shomburg I, Chang A, Shomburg D (2002) BRENDA, enzyme data and metabolic information. Nucleic Acids Res 30:47–9

Taquikhan MM, Martell AE (1962) Metal Chelates of Adenosine Triphosphate. J Phys Chem 66:10–5

Torres JC, Babul J (1991) An *in vitro* model showing different rates of substrate cycle for phosphofructokinases of *Escherichia coli* with different kinetic properties. Eur J Biochem 200(2):471–6

Vinopal RT, Fraenkel DG (1974) Phenotypic suppression of phosphofructokinase mutations in *Escherichia coli* by constitutive expression of the glyoxylate shunt. J Bacteriol 118(3): 1090–100

Vinopal RT, Fraenkel DG (1975) *PfkB* and *pfkC* loci of *Escherichia coli*. J Bacteriol 122(3): 1153–61

Waygood EB, Sanwal BD (1974) The control of pyruvate kinases of *Escherichia coli*. I. Physicochemical and regulatory properties of the enzyme activated by fructose 1,6-diphosphate. J Biol Chem 249(1):265–74

Wright JA, Sanwal BD (1971a) Regulatory Mechanisms involving nicotinamide adenine nucleotides as allosteric effectors. J Biol Chem 246:1689–99

Wright JA, Sanwal BD (1971b) Regulatory mechanisms involving nicotinamide adenine nucleotides as allosteric effectors. IV. Physicochemical study and binding of ligands to citrate synthase. J Biol Chem 246(6):1689–99